

THE THEORETICAL ANALYSIS OF H₂O-LiBr ABSORPTION REFRIGERATION SYSTEM USING AL₂O₃ NANOPARTICLES

JAGDISH S. TALPADA¹ & P. V. RAMANA²

¹Department of Mechanical Engineering, C.S. Patel Institute of Technology,
Charusat University, Changa, Anand, Gujarat, India

²Department of Mechanical, Sardar Vallabhbhai Patel Institute of Technology,
Vasad, Anand, Gujarat, India

ABSTRACT

The objective of this paper is to investigate the effect of nanoparticles on Coefficient of Performance (COP) of absorption refrigeration system using H₂O-LiBr by varying the generator, condenser and absorber temperature. The effect of nanoparticles on heat load of generator, condenser, evaporator and absorber at different operating temperatures was also studied in this work. The thermodynamic properties of H₂O-LiBr solution were coded using Energy Equation Solver (EES) software. The result shows that COP and heat loads of a system with nanoparticles at different operating temperatures follow the same trend as a base fluid system. The COP of a system with nanoparticles at each operating temperature is higher than the base fluid system. The heat supplied to the generator with nanoparticles is less than the heat supplied to the generator without nanoparticles while heat rejected in condenser and absorber of a system with nanoparticles is higher than the system without nanoparticles at each operating temperature. The heat exchanged in evaporator of a system with nanoparticles is also higher than the system without nanoparticles at each operating temperature. The Coefficient of performance of the system was also investigated by varying the volume fraction of nanoparticles. We obtained maximum COP with 0.2% volume fraction of nanoparticles.

KEYWORDS: Absorption Refrigeration System, H₂O-LiBr, Coefficient of Performance, Heat Load, Nanoparticles, Operating Temperature & Volume Fraction

Received: Feb 25, 2019; **Accepted:** Mar 15, 2019; **Published:** Apr 17, 2019; **Paper Id.:** IJMPERDJUN201934

INTRODUCTION

Vapour absorption refrigeration system is the best alternative of a vapour compression refrigeration system which requires electricity and creates the problem of ozone layer depletion. The absorption refrigeration system has less running cost because no external work is required like vapour compression refrigeration system. Also absorption refrigeration system has less ozone layer depletion because CFC refrigerant is not used. In spite of above advantage of absorption refrigeration system it is not used for commercial purpose because of its low performance. So it is required to improve the performance of absorption refrigeration system. In the literature numbers of reviews are found out on technique to improve the performance of an absorption refrigeration system directly or indirectly. Abed et al., 2016 reviewed the research and development on the effect of subcomponents and supported components on single effect absorption refrigeration cycle. They have presented the effects of distillation column inside the generator, adding rectifier, adding solution (refrigerant) heat exchangers and ejector on performance of the absorption cooling cycle. They have also summarized and reported the research and

development on re-arrangement of cycle, streamlines new working fluid and addition of nanoparticles. In literature many authors have suggested the modification of absorption refrigeration cycle to enhance the performance of an absorption refrigeration system (Talpada and Ramana, 2017). The design of various types of absorption refrigeration systems which increase the performance were reviewed by Srihirin et al., 2000. Literature on different solar thermal refrigeration systems, with a specific focus on solar absorption refrigeration systems and solar adsorption refrigeration systems within various working fluids is reviewed by Ullah et al., 2013. Bhargav et al., 2018 reported that hybridizing of the solar water heater with adsorption refrigerator can satisfy water heating and food preservation requirement.

The performance of an absorption refrigeration system is improved by the addition of nanoparticle in working pair. Many researchers have studied the effect of nanoparticles on the performance of absorption refrigeration system. Cheng and Liu, 2012 have made comprehensive review of nucleate boiling, flow boiling, condensation and two phase flow of refrigerant-based nanofluids. They have discussed the applications and challenges of refrigerant-based nanofluids. Nair et al., 2016 have reviewed researches on preparation of nano-refrigerant, thermophysical properties of nano-refrigerant, pressure drop in nano-refrigerant, boiling heat transfer of nano-refrigerant and performance of nano-refrigerant in domestic refrigerator. They concluded that the COP of refrigerating system is increased using nano-refrigerant and the thermal conductivity of nano-refrigerant is improved because of greater boiling heat transfer coefficient by the addition of nanoparticles. Also the high pressure drop takes place in nano-refrigerating system because of higher viscosity of nano-refrigerant which is surpassing with grater heat transfer performance of system.

The binary fluid of absorption refrigeration system requires good heat transfer and absorption properties for better performance. The literature survey shows the following results related to heat transfer rate, thermal conductivity and absorption rate with the addition of nanoparticles in binary fluid.

- The heat transfer rate is improved by the addition of nanoparticle in binary fluid, which is known as nano-refrigerant or nanofluid (Kang et al., 2008, Yang et al., 2012, Chen et al., 2014, Torii and Yoshino, 2015). The critical heat flux is increased about 200% using nanoparticles in pool boiling heat transfer (You et al., 2003).
- The basefluid with nanoparticles improves the thermal conductivity three times higher than conventional basefluid so it gives higher heat transfer rate with less increasing pumping power in heat transfer equipment (Choi et al., 1995, Martínez, 2013, Mahbubul et al., 2013, Fadhilah et al., 2014, Cuenca et al., 2014). The thermal conductivity of nano-refrigerant increases with increase of nanoparticle concentration and decreases with increase in particle size (Mahbubul et al., 2013).
- The absorption rate in the absorber is enhanced by the addition of nanoparticles because the absorption performance depends on the heat and mass transfer mechanism (Kang et al., 2000, Kim et al., 2007, Ki et al., 2010). The dispersion of nanoparticles in refrigerant enhances the absorption performance up to 3.21 times (Kim et al., 2006, Kim et al., 2007). Also the rate of absorption increases as the nanoparticles concentration is increasing (Kim et al., 2006, Kang et al., 2000). The use of binary nanofluid can reduce the size of absorber up to 54.4% (Kim et al., 2007).
- The viscosity of nano-refrigerant increases with increase of nanoparticle concentration. The frictional pressure drop and pumping power increases with particle concentration. The flow boiling heat transfer coefficient and convection heat transfer coefficient improves with nanoparticle concentration (Mahbubul et al., 2013).

Based on the above results, there are few studies carried out using nanoparticle in absorption refrigeration system to improve the performance. Mariappan and Udayakumar, 2013 have studied the effect of AL₂O₃ nanoparticles on heat transfer and absorption characteristic by varying generator temperature and nanofluids concentration. In this study they have considered R134a as a refrigerant and DMAC (Dimethyl Acetamide) with AL₂O₃ nanoparticles as absorbent. Their experiment results show that COP of the system is increased up to 18% at 80°C generator temperature. The heat duty of absorber is reduced about 22% at 60°C absorber temperature. The mass flow rate of strong solution required for the system decreases as the concentration of AL₂O₃ nanoparticles increases. Gulati et al., 2013 have reported with experimental study that the performance of the NH₃-H₂O absorption refrigeration cycle is enhanced by seeding AL₂O₃ nanoparticles directly in the generator due to the absorption and scattering effects of nanoparticles. Sözen et al., 2014 conducted an experiment to improve the performance of the diffusion absorption refrigeration system using AL₂O₃ nanoparticles. They reported that nanoparticle enhanced performance of the system due to better heat absorption in generator and increased evaporation in the evaporator.

In this paper, the theoretical analysis of the H₂O-LiBr absorption system with AL₂O₃ nanoparticles has been carried out. AL₂O₃ nanoparticles have been used to improve the performance of the system. Coefficient of performance and heat load of the main components of the system using AL₂O₃ nanoparticles have been calculated and compared with conventional systems to provide data for application of nanoparticles in absorption refrigeration system.

DESCRIPTION OF SYSTEM

Generator, absorber, pump, condenser, evaporator and expansion valve are the main components of absorption refrigeration system. Working of Vapour Absorption Refrigeration is as follows:

Liquid refrigerant (water) is receiving heat from surrounding and converted into vapour form in the evaporator. The vaporized refrigerant is absorbed in absorber by LiBr absorbent / water-LiBr weak solution. The re-absorption process is exothermic. The heat generated is removed from the absorber by supplying cooling water so that higher absorption rate is achieved.

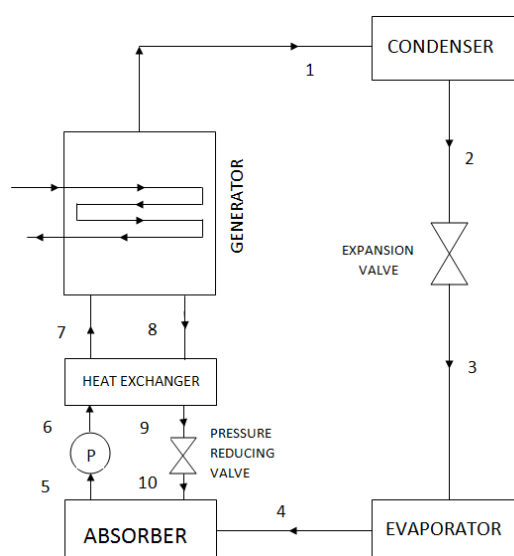


Figure 1: Schematic Diagram of Absorption Refrigeration Rig

The solution now rich (strong) in refrigerant (water) is pumped into the generator where heat is supplied to the

strong solution. Generally heat exchanger is used between generator and absorber to improve the performance of absorption refrigeration system. In heat exchanger weak solution of water – LiBr is heated by strong solution of water – LiBr.

In generator strong solution is heated so vaporization of refrigerant (water) takes place. Then vapour refrigeration is condensed in the condenser by supplying cooling water. The remaining weak solution in generator is supply back to the absorber through a pressure reducing valve. Liquid refrigerant coming from the condenser expanding through an expansion valve flows into the evaporator wherein cooling is achieved by evaporation of refrigerant.

SIMULATION AND ANALYSIS

Absorption Refrigeration System with H₂O / LiBr Working Pairs

The following set of input parameters are used to carry out simulation of water – LiBr absorption refrigeration system.

Evaporator temperature, t_e , °C

Generator temperature, t_g , °C

Absorber temperature t_a , °C

Condenser temperature, t_c , °C

Solution heat exchanger effectiveness, e

Nanoparticle volume fraction, ϕ

Refrigeration load Q_e , kcal/hr

In this analysis pump work, pressure drop in components and lines is neglected. Also at state 5, 8, 2 and 4 in figure 1 is assumed saturation conditions. The other properties are determined as follows:

Absorber Concentration

The absorber concentration at point 5, 6 and 7 is calculated using following equation at evaporator pressure P_e (Lansing [26])

$$X_5 = X_6 = X_7 = \frac{1.125t_a + 49.04 - t_e}{134.65 + 0.47t_a} \text{ kg /kg solution} \quad (1)$$

Generator Concentration

The generator concentration at point 8, 9 and 10 is calculated using following equation at condenser pressure P_c (Lansing [26]):

$$X_8 = X_9 = X_{10} = \frac{1.125t_g + 49.04 - t_c}{134.65 + 0.47t_g} \text{ kg /kg solution} \quad (2)$$

It may be noted that in evaporator and condenser pure water is flowing so values of X_1 , X_2 , X_3 and X_4 are zero

kg/kg solution.

Condenser and Evaporator Pressure

Condenser pressure, $P_c = P_6 = P_7 = P_8 = P_9 = P_{11} = P_2$ in mm Hg is calculated by following equation (Lansing [26]):

$$\log_{10} P_c = 7.8553 - \frac{1555}{t_c - 273.15} - \frac{11.2414 \times 10^4}{(t_c + 273.15)^2} \quad (3)$$

and Evaporator pressure, $P_e = P_5 = P_{10} = P_3 = P_4$ in mm Hg is calculated by following equation (Lansing [26]):

$$\log_{10} P_e = 7.8553 - \frac{1555}{t_e - 273.15} - \frac{11.2414 \times 10^4}{(t_e + 273.15)^2} \quad (4)$$

Mass Flow Rates

The flow rate of refrigerant is calculated by

$$m_r = \frac{Q_e}{h_4 - h_2} \quad (5)$$

Where

Q_e = refrigeration effect or cooling load

$h_3 = h_2$ = Saturated liquid refrigerant enthalpy

h_4 = Saturated vapour refrigerant enthalpy

Saturated liquid refrigerant (water) enthalpy h_2 is determined by following equation (Lansing [26])

$$h_2 = (t_c - 25) \text{ kcal/kg} \quad (6)$$

Saturated vapour refrigerant (water vapour) enthalpy h_4 is calculated by following equation (Lansing [26])

$$h_4 = 572.8 + 0.417 t_e \text{ kcal/kg} \quad (7)$$

The mass flow rate of weak solution and strong solution is calculated by following equations (Lansing [26]):

$$m_w = m_r \left(\frac{X_5}{X_8 - X_5} \right) \quad (8)$$

$$m_s = m_r \left(\frac{X_8}{X_8 - X_5} \right) \quad (9)$$

Solution Heat Exchanger Temperatures

The specific heat of water – LiBr strong solution (C_{X5}) having X_5 concentration, is determined by (Lansing [26])

$$C_{X5} = 1.01 - 1.23 X_5 + 0.48 X_5^2 \quad (10)$$

The specific heat of water – LiBr weak solution (C_{X8}) having X_8 concentration, is determined by (Lansing [26])

$$C_{X8} = 1.01 - 1.23 X_8 + 0.48 X_8^2 \quad (11)$$

Temperature at point 7 and 9 is calculated by following equations (Lansing [26]):

$$t_9 = t_g - e(t_g - t_a) \quad (12)$$

$$t_7 = t_a + \left[e \left(\frac{X_5}{X_8} \right) \left(\frac{C_{X8}}{C_{X5}} \right) (t_g - t_a) \right] \quad (13)$$

The enthalpies h_5 and h_9 are then calculated using following equations (Lansing, 1975):

$$h_5 = (42.81 - 425.92 X_5 + 404.67 X_5^2) + (1.01 - 1.23 X_5 + 0.48 X_5^2) t_a \quad (14)$$

$$h_9 = (42.81 - 425.92 X_8 + 404.67 X_8^2) + (1.01 - 1.23 X_8 + 0.48 X_8^2) t_9 \quad (15)$$

Heat transfer in Components

The heat balance of the condenser gives

$$Q_c = m_r (h_1 - h_2) \quad (16)$$

In term of specific heat above equation given by

$$Q_c = m_r C_{pv} t_g - m_r C_{pl} t_c \quad (17)$$

Where

C_{pv} = specific heat of vapour at generator temperature and pressure

C_{pl} = specific heat of liquid (water) at generator temperature and pressure

Heat transfer in generator (with heat exchanger) given by

$$Q_g = m_w h_9 + m_r h_1 - m_s h_6 \quad (18)$$

Heat transfer in absorber given by

$$Q_a = m_w h_{10} + m_r h_4 - m_s h_5 \quad (19)$$

So,

$$Q_a = m_w C_{X8} t_g + m_r C_{Pv} t_g - m_s C_{X5} t_7 \quad (20)$$

Coefficient of Performance (COP)

COP is calculated by following equation with neglecting pump work

$$COP = \frac{Q_e}{Q_g} \quad (21)$$

Absorption Refrigeration System with H₂O-AL₂O₃/LiBr

The COP of H₂O-AL₂O₃/LiBr system is calculated by equation (21). In this equation value of Q_g is calculated by using specific heats at the system pressure. The specific heat of the nano-refrigerant and water solution is calculated in two steps.

Firstly specific heat of the nanoparticles and refrigerant mixture is calculated and this data is used to calculate the specific heat of nano-refrigerant and water solution

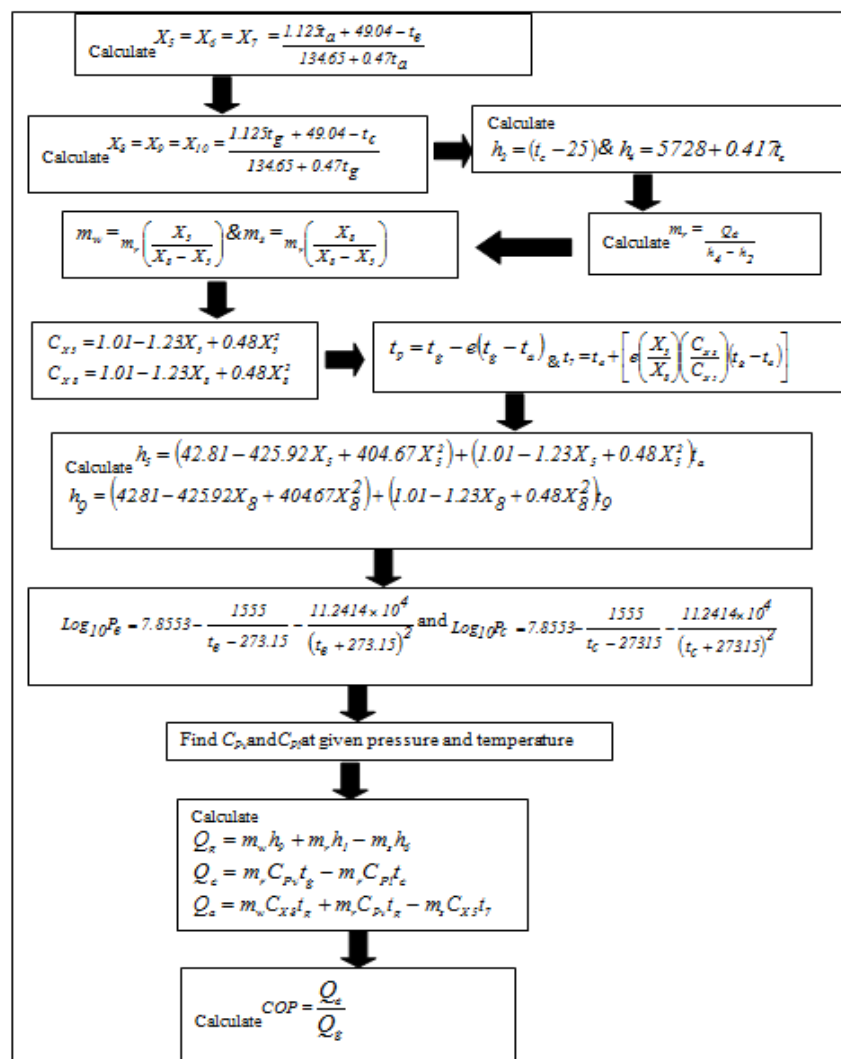
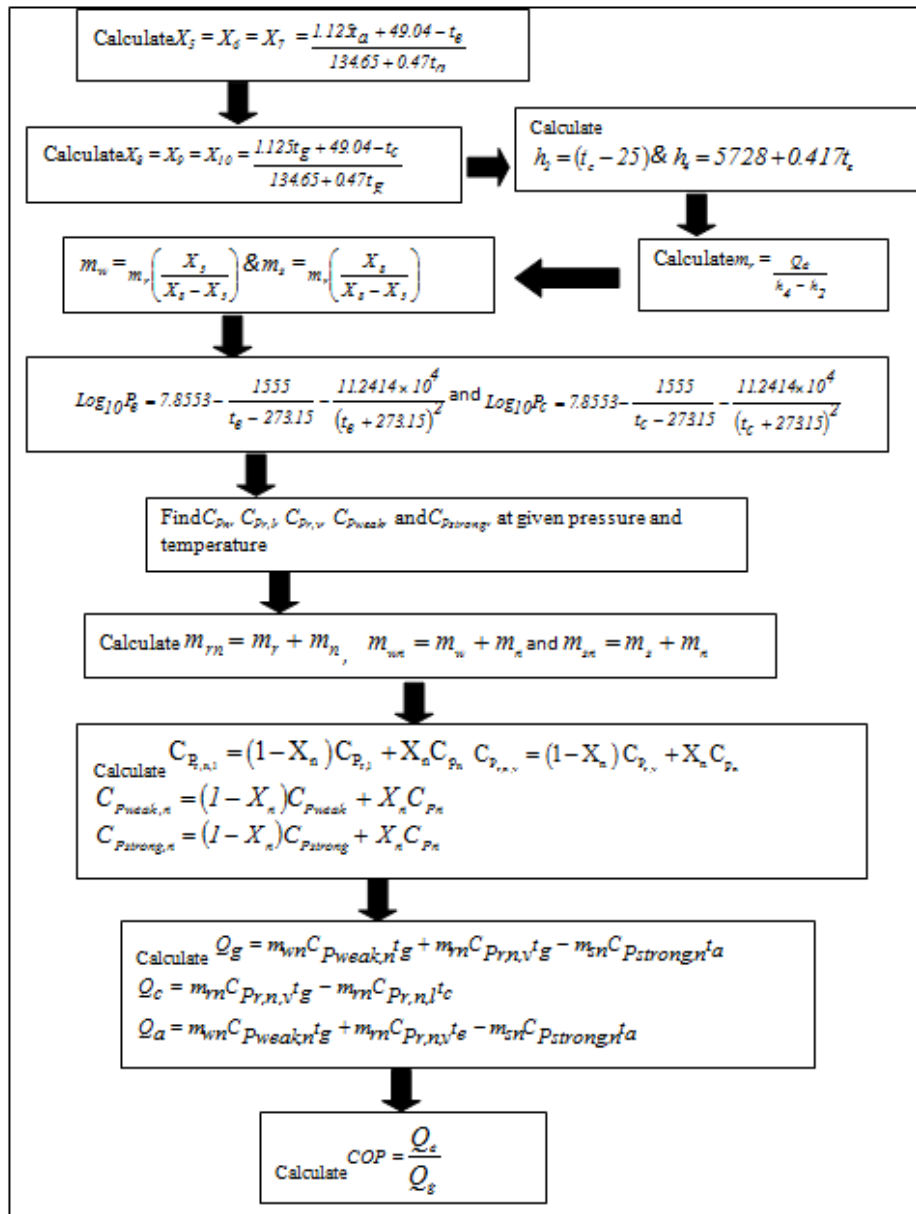


Figure 2: Calculation Flow Chart of H₂O / LiBr Working Pairs

Figure 3: Calculation Flow Chart of H₂O-AL₂O₃ / LiBr Working Pairs

Calculation of the Specific heat of Nano-Refrigerant

The following correlation is used to calculate the specific heat of nano-refrigerant (Mahbubul et al., 2013)

Specific heat of the liquid nano-refrigerants

$$C_{p,r,n} = (1 - X_n)C_{p,r} + X_nC_{p,n} \quad (22)$$

Take

$$X_n = \frac{m_n}{m_n + m_r} \quad (23)$$

Where,

m_n = mass of nano particles (AL₂O₃)

m_r = mass of refrigerant (H₂O)

Specific heat of the vapournano-refrigerants

$$C_{P_{r,n,v}} = (1 - X_n) C_{P_{r,v}} + X_n C_{P_n} \quad (24)$$

Specific heat of the weak solution with nanoparticles

$$C_{P_{weak,n}} = (1 - X_n) C_{P_{weak}} + X_n C_{P_n} \quad (25)$$

Specific heat of the strong solution with nanoparticles

$$C_{P_{strong,n}} = (1 - X_n) C_{P_{strong}} + X_n C_{P_n} \quad (26)$$

Take

$$m_{rn} = m_r + m_n \quad (27)$$

$$m_{wn} = m_w + m_n \quad (28)$$

$$m_{sn} = m_s + m_n \quad (29)$$

$$Q_c = m_{rn} C_{P_{r,n,v}} t_g - m_{rn} C_{P_{r,n,l}} t_c \quad (30)$$

$$Q_g = m_{wn} C_{P_{weak,n}} t_g + m_{rn} C_{P_{r,n,v}} t_g - m_{sn} C_{P_{strong,n}} t_a \quad (31)$$

$$Q_a = m_{wn} C_{P_{weak,n}} t_g + m_{rn} C_{P_{r,n,v}} t_e - m_{sn} C_{P_{strong,n}} t_a \quad (32)$$

VALIDATION OF MODEL

The EES model is validated by comparing simulation results with Somers et al. 2011 and BoonritPrasartkaew, 2014. The comparative studies of COP are shown in table1 and figure 4. The simulation result shows that as generator temperature increases, COP first increases and then decreases. The simulation result with EES shows maximum 1.8% discrepancy with the ASPEN prediction result which is carried out by Somers et al. 2011. Also, it shows good agreement with results of BoonritPrasartkaew, 2014. The variation in result is occurs due to practically less heat transfer in heat exchangers.

Table 1: Validation of EES Model with ASPEN

Parameter	ASPEN Prediction by C. Somers et al.	EES-Prediction by F. LANCING EQUATIONS	Difference (%)
Evaporator pressure (low pressure) (kPa)	0.6715	0.6636	1.17
Condenser pressure (high pressure) (kPa)	7.4606	7.461	0.005
Strong solution Concentration (%)	57.4	56.34	1.8
Weak solution Concentration (%)	62.57	62.17	0.6
Generator heat load, Q_g (kW)	14.592	14.855	1.8
Absorber heat load, Q_a (kW)	13.923	14.1006	1.3
Condenser heat load, Q_c (kW)	11.432	11.5266	0.8
Evaporator heat load, Q_e (kW)	10.772	10.772	n/a
COP	0.738	0.7251	1.7

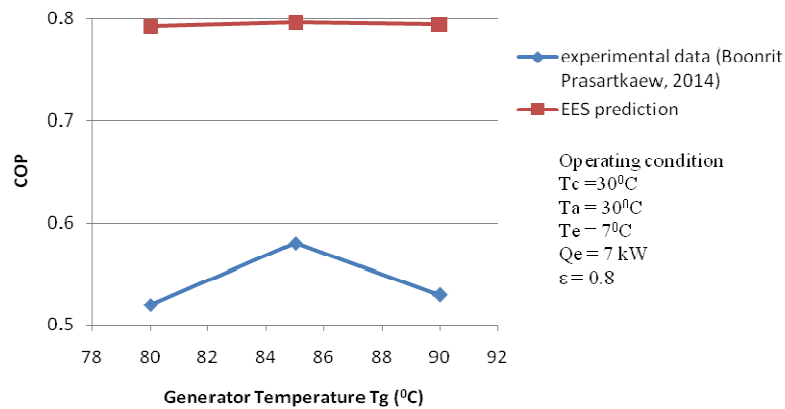


Figure 4: Validation of EES Model with Experimental Data

RESULT AND DISCUSSIONS

The following inlet conditions were considered for calculation of the heat transfer rates and COP.

Evaporator temperature, $t_e = 5^{\circ}\text{C}$

Absorber temperature $t_a = 30^{\circ}\text{C}$

Condenser temperature, $t_c = 30^{\circ}\text{C}$

Generator temperature, $t_g = 85^{\circ}\text{C}$

Solution heat exchanger effectiveness, $e = 0.8$

Nanoparticle volume fraction, ϕ or $X_n = 0.02$

Refrigeration load, $Q_e = 1512 \text{ Kcal/hr}$

Energy Equation Solver (EES) software is used to evaluate the performance of systems. The calculation flow chart for both working pair is shown in figure 2 and 3. The calculation results show that equations given in section 3 and 4

gives proper result for following temperature ranges.

To calculate COP and Heat supplied to Generator (Q_g):

Generator temperature: 87 °C – 120 °C.

Condenser temperature: 20 °C – 30 °C

Absorber temperature: 20 °C– 30 °C

To calculate Heat transferred in Condenser (Q_c) and Heat transferred in Absorber (Q_a):

Generator temperature: 80 °C – 120 °C

Condenser temperature: 20 °C – 30 °C

Absorber temperature: 20 °C – 30 °C

So the effects of operating temperatures (generator temperature, condenser temperature and absorber temperature) on COP and heat transfer in main components of system with nanoparticles are studied for above ranges and compared with basefluid system. The results of studied are as follows:

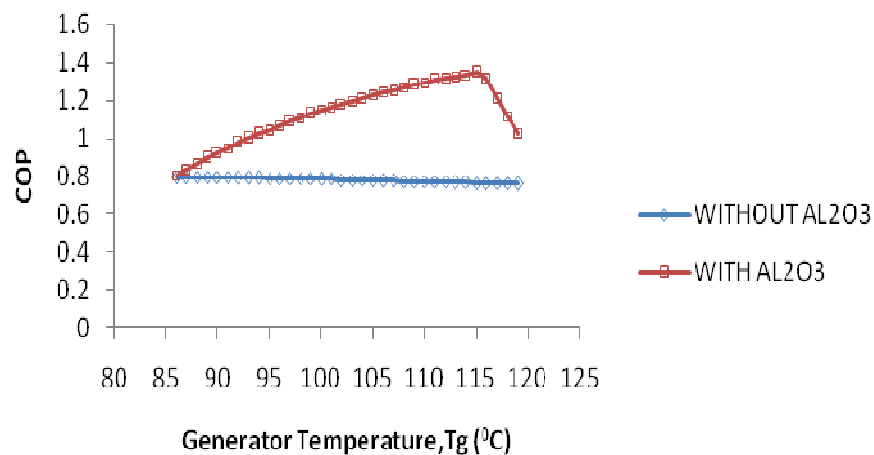


Figure 5: Generator Temperature (Tg) vs COP

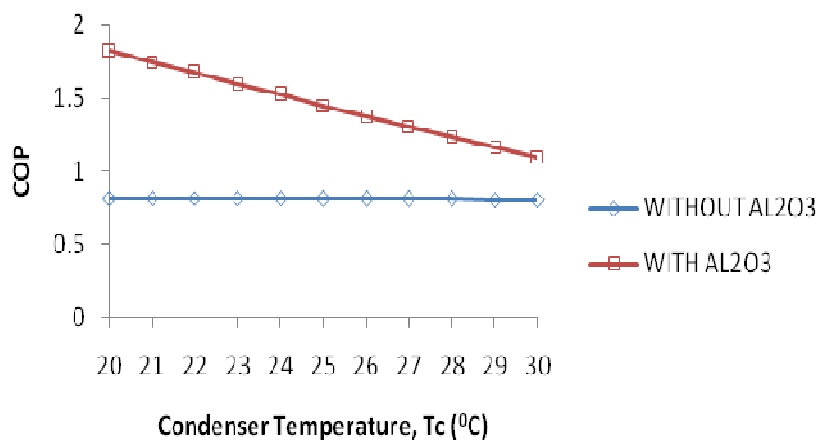


Figure 6: Effect of Condenser Temperature on COP

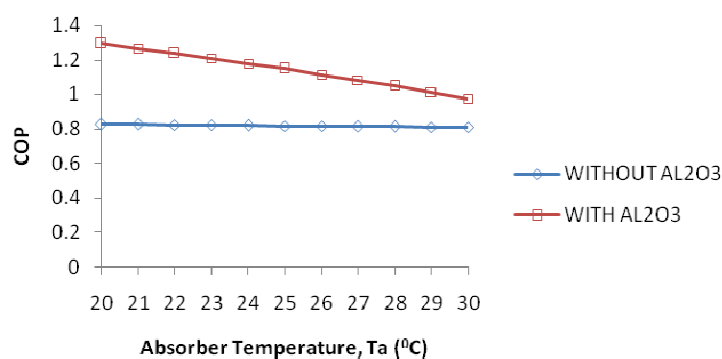


Figure 7: Effect of Absorber Temperature on COP

Effect of Nanoparticles and Operating Temperatures on COP

Figures 5, 6 and 7 show the variation of the COP with operating temperatures. The comparison of Coefficient of Performance values at different generator temperature for system with and without Al_2O_3 nanoparticles are shown in figure 5. It can be seen that COP increases with generator temperature for both systems. Figure 6 shows the variation of the COP with condenser temperature. It is observed that COP decreases with condenser temperature. Also COP decreases with absorber temperature as shown in figure 7.

The results also show that the COP values of system with Al_2O_3 nanoparticles are higher and vary faster than the base fluid system at each generator, condenser and absorber temperature. The reason is that the heat transfer rate is increase using nanoparticles so it required less heat to attain the same generator temperature. The addition of nanoparticles increases the COP by 1-35% under set generator temperature range, by 35-124% under set condenser temperature range and 20-56% under set absorber temperature range.

Effect of Nanoparticles and Operating Temperature on Thermal Loads

Figure 8, 9 and 10 show the effect of generator, condenser and absorber temperature on heat supplied to the generator (Q_g). It can be seen that the heat supplied to generator increases with a generator and absorber temperature for systems with and without Al_2O_3 nanoparticles (figure 8 and 10). Figure 9 shows that the heat supplied to generator decreases as condenser temperature increases. It is observed that at set generator temperature range, heat required in generator of the system using Al_2O_3 nanoparticles decreases by 1-43%, whereas heat required in generator is reduced by 26-55% under set condenser temperature range and by 17-36% under set absorber temperature range. This reduction is due to the addition of nanoparticles, which increase heat and mass transfer characteristic of binary solution.

Figure 11, 12 and 13 show the variation of heat rejection in condenser (Q_c) at a different generator, condenser and absorber temperature with and without Al_2O_3 nanoparticles. The heat rejection in condenser (Q_c) increases with generator temperature (figure 11) while it decreases with condenser temperature for both type of working fluid (figure 12). The Q_c is not much influenced by variation of absorption temperature with and without nanoparticles as shown in figure 13. The Q_c is increased by 1-2% under set generator temperature range and condenser temperature range. Also Q_c increases by 1.5% under given absorber temperature range.

The variation of heat rejected in absorber (Q_a) with generator, condenser and absorber temperature is shown in figure 14, 15 and 16. It is observed that Q_a increases as the generator temperature increase for system without nanoparticles while for system with nanoparticles it first decreases to minimum then increases with generator temperature

(figure 14). The Q_a increases with condenser and absorber temperature for both systems (figure 15 and 16). The values of Q_a for a nanofluid base system are higher than the base fluid system at each operating temperature. The Q_a increases minimum 4% at 115°C generator temperature while it increases minimum 16% at 20°C condenser temperature and minimum 82% at 20°C absorber temperature.

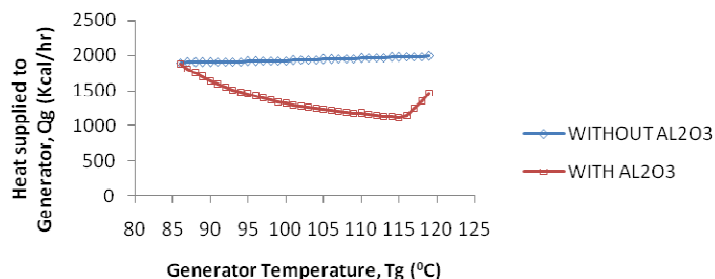


Figure 8: Effect of Generator Temperature on Heat Supplied to the Generator

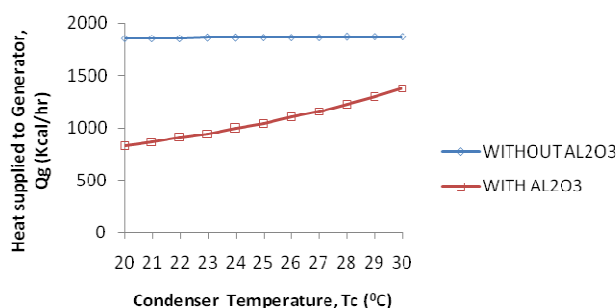


Figure 9: Effect of Condenser Temperature on Heat Supplied to the Generator

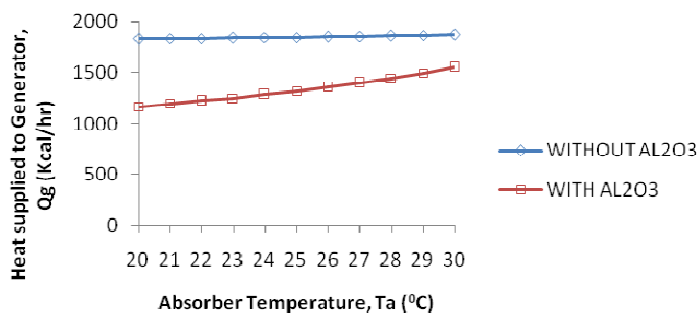


Figure 10: Effect of Absorber Temperature on Heat Supplied to the Generator

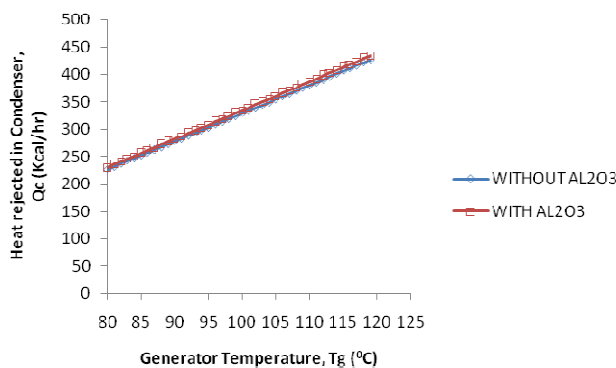


Figure 11: Effect of Generator Temperature on Heat Rejected in Condenser

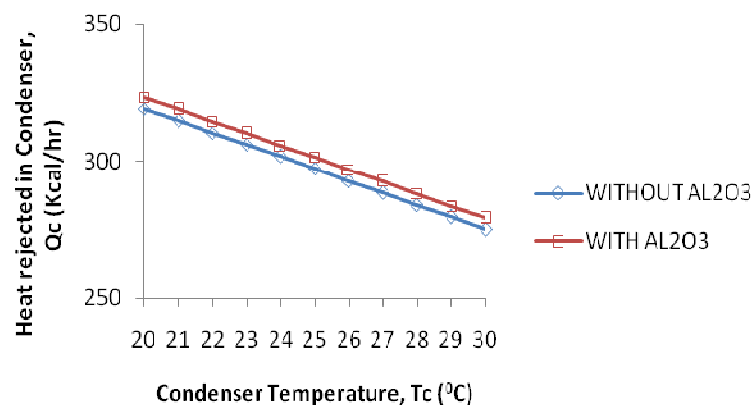


Figure 12: Effect of Condenser Temperature on Heat Rejected in Condenser

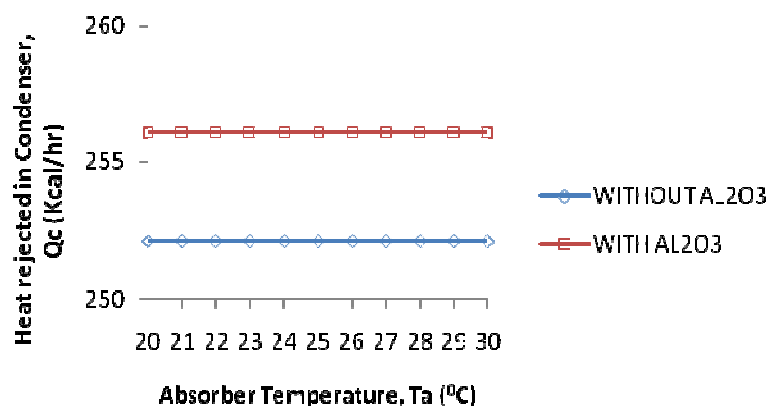


Figure 13: Effect of Absorber Temperature on Heat Rejected in Condenser

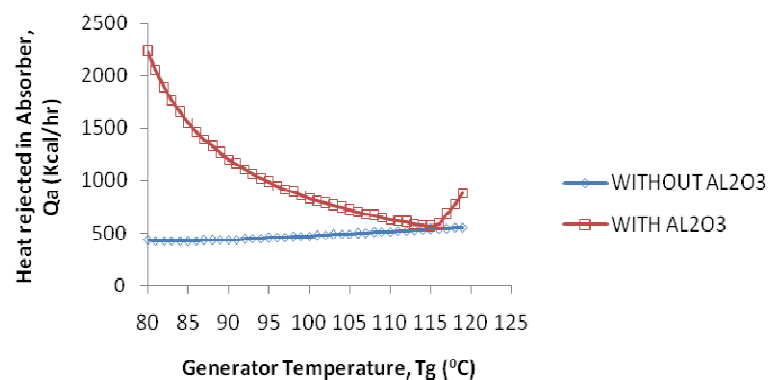


Figure 14: Effect of Generator Temperature on Heat Rejected in Absorber

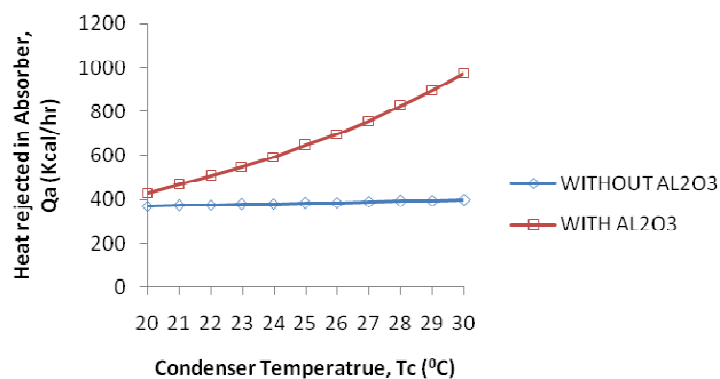


Figure 15: Effect of Condenser Temperature on Heat Rejected in Absorber

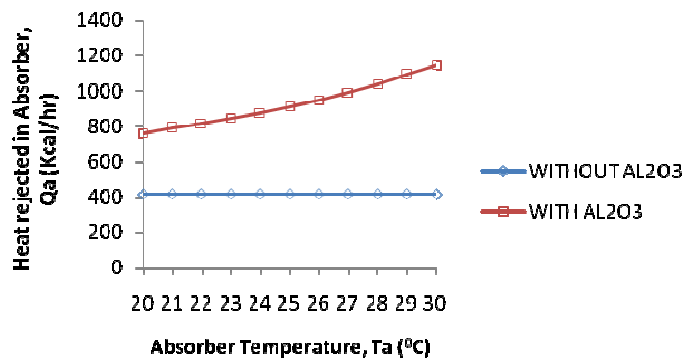


Figure 16: Effect of Absorber Temperature on Heat Rejected in Absorber

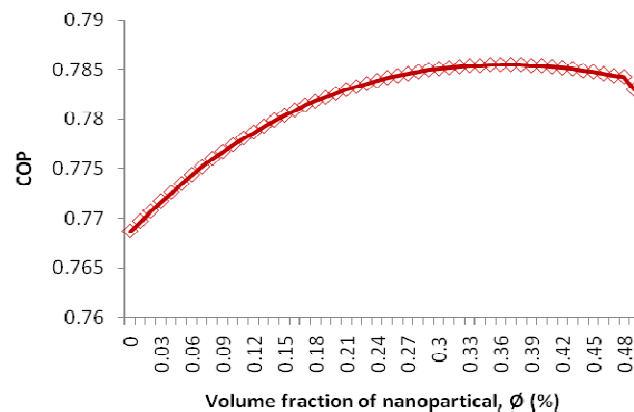


Figure 17: Effect of Volume Fraction of Nanoparticle on COP

Effect of Nanoparticle Concentration

Figure 17 shows the effect of volume fraction of nanoparticles on COP . The result shows that as the volume fraction of nanoparticles is increased, first the COP of the system increases and then decreases. It can be seen that the maximum COP of system is about 0.7855 with 0.35% volume fraction of nanoparticles.

CONCLUSIONS

The theoretical analysis of the H_2O -LiBr absorption refrigeration system was carried out in this study. The operating temperature ranges of the system, to carry out experiment, were set within the following ranges:

For COP and Heat supplied to Generator (Q_g) calculation:

Generator Temperature: $87^\circ C - 120^\circ C$.

Condenser Temperature: $20^\circ C - 30^\circ C$

Absorber Temperature: $20^\circ C - 30^\circ C$

For Heat transfer in Condenser (Q_c) and Heat transfer in Absorber (Q_a) calculation:

Generator Temperature: $80^\circ C - 120^\circ C$

Condenser Temperature: $20^\circ C - 30^\circ C$

Absorber Temperature: $20^\circ C - 30^\circ C$

The following conclusions are derived from the present theoretical study.

- The *COP* and thermal loads of a system with nanoparticles are follows the same trends as base fluid systemat different operating temperatures but vary with faster rate.
- The *COP* of a system with nanoparticles is higher than the base fluid systemat each operating temperature. The addition of nanoparticles increases the *COP* by 1-35% under generator temperature range, by 35-124% under condenser temperature range and by 20-56% under absorber temperature range.
- The thermal load of generator of a system with nanoparticles is less than the base fluid system at all operating temperatures. Heat supplied to the generator (Q_g) for the system using nanoparticlesdecreases by 1-43% under generator temperature range while decreases by 26-55% under condenser temperature range and by 17-36% under absorber temperature range.
- Heat rejection in condenser (Q_c) increases with the addition of nanoparticles in binary fluid. The value of Q_c increases by 1-2%, 1-2% and 1.5% under generator, condenser and absorber temperature ranges respectively.
- Also heat rejected in absorber (Q_a) with nanoparticles is higher than without nanoparticles. The value of Q_a increases as the generator temperature increases for system without nanoparticles while for system with nanoparticles it first decreases to minimum then increases with generator temperature. The Q_a increases with condenser and absorber temperature for both systems.
- The maximum *COP* of the system is achieved with 0.2% volume fraction of nanoparticles.
- Finally, the experimental analysis of an absorption refrigeration system with and without nanoparticles clearly shows that the absorption refrigeration system with nanofluid have better performance.

NOMENCLATURE

<i>COP</i>	Coefficient of Performance
Q_g	Heat supplied to Generator, kcal/hr
Q_c	Heat rejected in Condenser, kcal/hr
Q_e	Heat exchanged in Evaporator, kcal/hr
Q_a	Heat rejected in Absorber, kcal/hr
t	Temperature, °C
t_g	Generator Temperature, °C
t_a	Absorber Temperature, °C
t_c	Condenser Temperature, °C
t_e	Evaporator Temperature, °C
X	solution concentration, kg libr/kg solution
C_x, C_p	specific heat, kcal/kg°C
m_r	mass flow rate of refrigerant, kg/hr
m_s	mass flow rate of strong solution, kg/hr
m_w	mass flow rate of weak solution, kg/hr
ε	heat exchanger effectiveness

ACKNOWLEDGEMENTS

The authors would like to thank the Department of Mechanical Engineering, CPIT, Changa for all the support and encouragement.

REFERENCES

1. Abed AM, Alghoul MA, Sopian K, Sh H, Al-shamani AN, Muftah AF. Enhancement aspects of single stage absorption cooling cycle : A detailed review. *Renew Sustain Energy Rev* 2016;1–36. doi:10.1016/j.rser.2016.11.231.
2. Talpada JS, Ramana P V. A review on performance improvement of an absorption refrigeration system by modification of basic cycle. *Int J Ambient Energy* 2018. doi:10.1080/01430750.2017.1423379.
3. Sriksirin P, Aphornratana S, Chungpaibulpatana S. A review of absorption refrigeration technologies. *Renew Sustain Energy Rev* 2000;5:343–72. doi:10.1016/S1364-0321(01)00003-X.
4. Ullah KR, Saidur R, Ping HW, Akikur RK, Shuvo NH. A review of solar thermal refrigeration and cooling methods. *Renew Sustain Energy Rev* 2013;24:499–513. doi:10.1016/j.rser.2013.03.024.
5. Bhargav H. Development of semi-continuous solar powered adsorption water chiller for food preservation. *J Therm Eng* 2018;4:2169–87. doi:10.18186/journal-of-thermal-engineering.434032.
6. Cheng L, Liu L. Boiling and two-phase flow phenomena of refrigerant-based nanofluids : Fundamentals, applications and challenges. *Int J Refrig* 2012;36:421–46. doi:10.1016/j.ijrefrig.2012.11.010.
7. Nair V, Tailor PR, Parekh AD. Nanorefrigerants:- a comprehensive review on its past, present and future. *Int J Refrig* 2016;67:290–307. doi:10.1016/j.ijrefrig.2016.01.011.
8. Kang YT, Kim HJ, Lee K Il. Heat and mass transfer enhancement of binary nanofluids for H₂O / LiBr falling film absorption process. *Int J Refrig* 2008;31:850–6. doi:10.1016/j.ijrefrig.2007.10.008.
9. Yang L, Du K, Bao S, Wu Y. Investigations of selection of nanofluid applied to the ammonia absorption refrigeration system. *Int J Refrig* 2012;35:2248–60. doi:10.1016/j.ijrefrig.2012.08.003.
10. Chen T, Kim J, Cho H. Theoretical analysis of the thermal performance of a plate heat exchanger at various chevron angles using lithium bromide solution with nanofluid. *Int J Refrig* 2014. doi:10.1016/j.ijrefrig.2014.08.013.
11. Torii S, Yoshino H. Effect of Aqueous Suspension of Graphene-Oxide Nanoparticles on Thermal Fluid Flow Transport in Circular Tube. *Int J Air-Conditioning Refrig* 2015;23:1550005. doi:10.1142/S2010132515500054.
12. You SM, Kim JH, Kim KH. Effect of nanoparticles on critical heat flux of water in pool boiling heat transfer Effect of nanoparticles on critical heat flux of water in pool boiling heat transfer. *Appl Phys Lett* 2003;83. doi:10.1063/1.1619206.
13. Choi, Stephen U S, Eastman, J.A. Enhancing Thermal Conductivity Of Fluids With Nanoparticles. *ASME Int Mech Eng Congr Expo* 1995.
14. Othman, A. A., Osman, M. A., Wahdan, M. H., & ABED-ELRAHIM, A. G. (2014). Thermal annealing and UV induced effects on the structural and optical properties of capping free ZnS nanoparticles synthesized by Co-precipitation method. *International Journal of General Engineering and Technology*, 3, 9-16.
15. Martínez YC. Experimental Study of Thermal Conductivity of New Mixtures For Absorption Cycles and The Effect of The Nanoparticles Addition. *Dr Thesis* 2013.
16. Mahbulul IM, Fadhilah SA, Saidur R, Leong KY, Amalina MA. Thermophysical properties and heat transfer performance of

- Al₂O₃/R-134a nanorefrigerants. Int J Heat Mass Transf* 2013;57:100–8. doi:10.1016/j.ijheatmasstransfer.2012.10.007.
17. Fadhilah SA, Marhamah RS, Izzat AHM. Copper Oxide Nanoparticles for Advanced Refrigerant Thermophysical Properties : Mathematical Modeling. *J Nanoparticles* 2014;2–7. doi:dx.doi.org/10.1155/2014/890751.
 18. Cuenca Y, Vernet A, Valle M. Thermal conductivity enhancement of the binary mixture (NH₃ + LiNO₃) by the addition of CNTs. *Int J Refrig* 2014;1:0–7. doi:10.1016/j.ijrefrig.2013.12.013.
 19. Kang YT, Kunugi Y, Kashiwagi T. Review of advanced absorption cycles : performance improvement and temperature lift enhancement. *Int J Refrig* 2000;23:388–401.
 20. Kim J, Akisawa A, Kashiwagi T, Tae Y. Numerical design of ammonia bubble absorber applying binary nanofluids and surfactants. *Int J Refrig* 2007;30:1086–96. doi:10.1016/j.ijrefrig.2006.12.011.
 21. Ki J, Koo J, Hong H, Tae Y, Nh HO. The effects of nanoparticles on absorption heat and mass transfer performance in NH₃ / H₂O binary nanofluids. *Int J Refrig* 2010;33:269–75. doi:10.1016/j.ijrefrig.2009.10.004.
 22. Rashid, F., Dawood, K., & Hashim, A. H. M. E. D. (2014). Maximizing of solar absorption by (TiO₂-water) nanofluid with glass mixture. *International Journal of Research in Engineering & Technology*, 2, 87-90.
 23. Kim JK, Jung JY, Kang YT. The effect of nano-particles on the bubble absorption performance in a binary nanofluid. *Int J Refrig* 2006;29:22–9.
 24. Kim JK, Jung JY, Kang YT. Absorption performance enhancement by nano-particles and chemical surfactants in binary nanofluids. *Int J Refrig* 2007;30:50–7. doi:10.1016/j.ijrefrig.2006.04.006.
 25. Mariappan V, Udayakumar M. Thermodynamic Analysis of R134a–Dmac Vapor Absorption Refrigeration (Var) System. *Int. Conf. Adv. Res. Mech. Aeronaut. Civ., Pattaya: 2013*, p. 59–64.
 26. Gulati R, Reddy A, Khullar V, Bhalla V, Tyagi H, Zhao Y, et al. International Journal of Environmental Enhancing the efficiency of absorption refrigeration cycle by “ seeding ” nanoparticles directly in the working fluid. *Int J Environ Stud* 2013;37–41. doi:10.1080/00207233.2013.798503.
 27. Sözen A, Özbaş E, Menlik T, Çakir MT, Gürü M, Boran K. Improving the Thermal Performance of Diffusion Absorption Refrigeration System with Alumina Nanofluids: An Experimental Study. *Int J Refrig* 2014. doi:10.1016/j.ijrefrig.2014.04.018.
 28. Bhagat, V. K., Prasad, A. K., & Srivastava, A. K. L. Influence of Moisture Absorption and their Effect on the Physio-Mechanical Properties of Coir-Luffa fibre Reinforced Polymer Matrix Composites.
 29. Lansing F. L. Computer Modeling of a Single -Stage Lithium Bromide/Water Absorption Refrigeration Unit. *JPL Deep Sp Netw Prog Rep* 42-32 1975:247–57.